

ORIGINAL RESEARCH

An observational analysis of the eastern tropical Pacific Shallow Meridional Circulation using YOTC data and pilot balloons from Isla del Coco, Costa Rica

GABRIELA MORA-ROJAS^{1, 2, *} and ERIC J. ALFARO^{1, 2, 3, 4}

¹Centro de Investigaciones Geofísicas (CIGEFIS), Universidad de Costa Rica (UCR), 11501-2060 San José, Costa Rica.

²Escuela de Física (EFIs), Universidad de Costa Rica (UCR), 11501-2060 - San José, Costa Rica. ³Centro de Investigación en Ciencias del Mar y Limnología (CIMAR), Universidad de Costa Rica (UCR), 11501-060 - San José, Costa Rica. ⁴Centro de Investigación en Matemática Pura y Aplicada (CIMPA), Universidad de Costa Rica (UCR), 11501-060 - San José, Costa Rica.

ORCID *Gabriela Mora-Rojas*  <https://orcid.org/0009-0001-4708-6193>, *Eric J. Alfaro*  <https://orcid.org/0000-0001-9278-5017>



ABSTRACT. The low-level circulation of the atmosphere over Isla del Coco has been studied and the presence of a northerly wind at low levels of the atmosphere in the eastern tropical Pacific, in addition to the deep Hadley circulation cell, has been confirmed. Using data from pilot balloons (May 1997 through January 1999, October 2007 through April 2008), the northern flow is between 1 and 5 km high, depending on the time of year, with a maximum speed located between 2 and 3 km above the surface. The generating mechanism of the surface return flow in the Hadley circulation cell has been formulated as a sea breeze, Ekman pumping of the boundary layer, and it could even be a response to the Rossby wave generated by warming in the Chocó region. These results agree with those obtained from the ERA5 reanalysis (January 1979 through December 2020), which show that the southern return cell varies in position and height during the course of the year, with a poorly organized circulation in March and strengthening from July to February. The incorporation of data of low, medium and high cloud cover from Year of the Tropical Convection (boreal summer 2009) evidenced the presence of high-level clouds in the ITCZ region and low-level clouds to the south of the ITCZ, latitudes where the south surface circulation cell is located.

Key words: Low-level atmosphere, Hadley circulation cell, Ekman pumping, ERA5, Central America, pilot balloons, Chocó region.



*Correspondence:
gabriela.morarojas@ucr.ac.cr

Received: 31 May 2023
Accepted: 13 December 2023

ISSN 2683-7595 (print)
ISSN 2683-7951 (online)

<https://ojs.inidep.edu.ar>

Journal of the Instituto Nacional de
Investigación y Desarrollo Pesquero
(INIDEP)



This work is licensed under a Creative
Commons Attribution-
NonCommercial-ShareAlike 4.0
International License

Un análisis observacional de la circulación meridional somera del Pacífico tropical oriental utilizando datos YOTC y globos piloto de la Isla del Coco, Costa Rica

RESUMEN. Se ha estudiado la circulación de la atmósfera en niveles bajos sobre la Isla del Coco y se ha confirmado la presencia de un viento del norte en los niveles bajos de la atmósfera en el Pacífico Oriental Tropical, además de la celda de circulación profunda de Hadley. Utilizando datos de globos piloto (mayo 1997 a enero 1999, octubre 2007 a abril 2008), el flujo del norte está entre 1 y 5 km de altura, dependiendo de la época del año, con una velocidad máxima situada entre 2 y 3 km sobre la superficie. El mecanismo generador del flujo de retorno superficial en la celda de circulación de Hadley ha sido formulado como una brisa marina, bombeo de Ekman de la capa límite, e incluso podría ser una respuesta a la onda de Rossby generada por el calentamiento en la región del Chocó. Estos resultados concuerdan con los obtenidos del reanálisis ERA5 (enero 1979 a diciembre 2020), que muestran que la celda de retorno sur varía en posición y altura a lo largo del año, con una circulación mal organizada en marzo y fortaleciéndose de julio a febrero. La incorporación de datos de nubosidad baja, media y alta del Año de la Convección Tropical (verano boreal 2009) evidenció

la presencia de nubes altas en la región de la ZCIT y nubes bajas al sur de la ZCIT, latitudes donde se encuentra la situada la celda de circulación superficial sur.

Palabras clave: Atmósfera de bajo nivel, celda de circulación de Hadley, bombeo de Ekman, ERA5, América Central, globos piloto, región del Chocó.

INTRODUCTION

The winter and summer hemisphere Hadley cells are relevant circulations of the tropical atmosphere. They consist of ascending motion close to the equator, divergent flow at upper tropospheric levels, convergent flow toward the Intertropical Convergence Zone (ITCZ) near the surface, and descending motion in the subtropics, as in the North Atlantic and Pacific subtropical highs (Amarador et al. 2006, 2016a). In addition to this deep circulation, there is a secondary circulation embedded on the deep Hadley circulation, known as Shallow Meridional Circulation or SMC (González and Mora-Rojas 2014).

This SMC is observed as a southerly flow at the lowest levels, with a shallow northerly return flow (SRF) between 1 and 5 km, in contrast to the well-known northerly flow of the deep Hadley circulation located within 10 and 12 km. Wang et al. (2005) found that the SMC in the eastern Pacific is strongest between 85° W and 125° W, with a tendency to become deeper toward the west, which seems to be correlated with the increase of the inversion height toward the west (von Ficker 1936; Neiburger et al. 1961). Its meridional extent also varies in the zonal direction. For example, east of 105° W, the SMC is confined between 5° S and the northern ITCZ, which occurs at approximately 10° N, whereas near 120° W the SMC penetrates to 15° S.

Shallow meridional circulations occur in other parts of the globe (Trenberth et al. 2000), for instance Africa, Middle East, Australia, the tropical eastern Pacific and Atlantic. The deep well-known Hadley circulation displays maximum magnitude

in July and a secondary maximum in January, whereas the second circulation is the lower-tropospheric overturning cell centered near 800 hPa. Trenberth et al. (2000) described two examples of this circulation. The first one was the regional meridional cross section of the divergent flow, averaged between 170° W and 90° W, for July, illustrating the simultaneous occurrence of deep and shallow Hadley cells. The second one, showed the regional meridional cross section of the divergent flow, averaged between 30° W and 10° E, for January, illustrating the occurrence of the shallow Hadley cell during a period when the deep Hadley cell is largely absent.

Several authors have provided observational insights into the role of sea surface temperature (SST) in boundary layer (BL) processes in the Eastern Tropical Pacific (ETPac) in the past. Lindzen and Nigam (1987) proposed a mechanism of meridional sea surface temperature (SST) gradients and resulting pressure gradients (Back and Bretherton 2009) to explain low-level winds in the BL trade cumulus, finding that SST's and its gradients are positively correlated in the vertical through the depth of the trade cumulus layer.

Wallace et al. (1989) and Deser et al. (1993) studied the meridional variations of the static stability upon the area over the cold tongue at 1° S and a frontal zone at 2° N, to understand the formation of stratiform clouds on the warm side of the front. When the northward-moving BL flow crosses northward upon the cold tongue at 1° S, high static stability (Chelton et al. 2001) inhibits the downward turbulent mixing of northward momentum from aloft. The low-level wind diverges over the SST frontal zone at 2° N (i.e. toward warmer waters) and the BL is destabilized, increasing turbulence and downward mixing of northward momen-

tum. Satellite images and SST data used by Deser et al. (1993) show that when the front is strong (weak), there is a maximum (minimum) of cloudiness. A strong (weak) front is found during cold (warm) the El Niño/Southern Oscillation (ENSO) episodes. The strong low-level southerly winds are influenced by the ENSO and the annual cycle (Amador et al. 2006, 2016a), displaying stronger flow during cold seasons, in particular during cold seasons of warm years. Furthermore, there is feedback between strong SST gradients forcing shallow cloudiness, and radiative cooling caused by cloudiness and subsequent strengthening of SST gradients (Amador et al. 2006). All these factors regulate the precipitation in the ITCZ region north of the equator (Amador et al. 2006, 2016a; Durán-Quesada et al. 2020).

Another aspect of the dynamics was noted earlier by Tomas and Webster (1997), who pointed out that strong cross-equatorial flow can lead to an area in the meridional plane, between the equator and the zero absolute vorticity at the surface, where the absolute vorticity has the opposite sign of the Coriolis parameter f , which is the condition for inertial instability.

Using data from EPIC 2001, McGauley et al. (2004) found the strongest meridional wind speed between 0° N and 5° N; however, these winds do not accelerate due to the forcing of the strong pressure gradient found in the boundary layer. The meridional pressure gradient changes its direction above 1 km at certain latitudes, resulting in the reversal of the meridional wind near 1,200 m of altitude and 5° N, where the northerlies are strongest.

Zhang et al. (2004) and Nolan et al. (2007) attributed the cause of the SMC to sea surface temperature (SST) gradients, comparing the SMC to a large-scale circulation resembling sea-breeze, driven by meridional SST gradients. The authors found a stronger SMC when the ITCZ does not display deep convection. Nolan et al. (2010) performed a study where the SRF is analyzed as a sea-breeze-like response to surface gradients of pressure and temperature, particularly near the equator. Wang

et al. (2005) and de Szoeke et al. (2005) used data from EPIC 2001 as well and found a weak return circulation during the boreal fall, located at 95° W and above the boundary layer. The authors also found most of the stratocumulus in a narrow area over the convective mixed layer, within 1° N and 3° N, while those found south of the equator are near the inversion base.

The treatment of the circulation between 10° S and 10° N as a sea-breeze circulation (Nolan et al. 2007) does not account for important mechanisms such as the variation of the Coriolis parameter with latitude, which causes important variations in the inertial stability. Vorticity in the region of the ITCZ produces Ekman pumping out the boundary layer (González and Mora-Rojas 2014). The most likely horizontal trajectory for this air is toward an area with low inertial stability, equatorward rather than poleward where the inertial stability β^{2y^2} is larger and this one more effectively retards the flow.

In other modeling results, the SMC could be a response to a Rossby wave generated at the heat source near El Chocó (Mesa-Sánchez and Rojo-Hernández 2020), which produces two cyclones converging into the heat source. The northern cyclone has negative vorticity, whereas the southern one is weaker and has positive vorticity. This positive cyclone is associated with the shallow convection nearby the main position of the SMC.

On the other hand, Huaman et al. (2021) analyzed data from the OTREC 2019 field campaign, and found interesting results about the existence, weakening or strengthening of the deep and shallow clouds and circulations at the transit of tropical easterly waves. The authors found intense convective activity while the cyclonic part of the tropical wave is passing over the region of the ITCZ, but at the pass of the anticyclonic part of the tropical wave at the second or third day, weak and shallow convection develops south of the ITCZ. This behavior has been explained by the vertically integrated moisture flux convergence (MFC). When the MFC convergence term is positive, the ITCZ is strong and the circulation is deep. When the MFC

convergence term is negative, deep convection is absent, and positive MFC advection from south of the ITCZ enhances a shallow circulation and convection. The moist static energy (MSE) was also used to study the shape of the vertical motion profile in the ITCZ. The horizontal advection of MSE is negative during deep convection, but positive and southward of the ITCZ when shallow convection is observed.

The meridional displacement of the ITCZ was studied by Kang et al. (2008) by using a GCM model coupled to a slab mixed layer ocean. Their experiment showed that by warming one hemisphere and simultaneously cooling the other through a cross-equatorial flux, subsidence would be present in the tropics of the cooled hemisphere, enabling the formation of the observed shallow clouds. The asymmetry between the Hadley cells in both hemispheres was also explored by Hack et al. (1989) and Hack and Schubert (1990) using dynamical arguments based on the Eliassen meridional circulation equation (with variable coefficients: static stability, baroclinicity and inertial stability), and by Schubert et al. (1991) based on potential vorticity dynamics. These dynamical arguments are quite different from those used by Lindzen and Hou (1988), since they are not based on a steady state assumption, but rather involve wind and mass fields that are evolving into states that satisfy the Charney-Stern necessary condition for combined barotropic-baroclinic instability.

Idealized analytical and numerical models of zonally symmetric flow have provided knowledge about the individual Hadley cells. For instance, Lindzen and Hou (1988) simulated the seasonal migration of these cells in response to the north-south migration of the sea surface temperature maximum. Their results show that, as the center of the heating moves off the equator, the latitude separating the winter and summer cells moves much further into the summer hemisphere while the summer cell becomes negligible. The summer cell is the one found in the hemisphere where the ITCZ is located, while the winter cell is found in the opposite

hemisphere. Using a high-resolution version of a numerical model, Hack et al. (1989) and González and Mora-Rojas (2014) found that when the heat source is at 2° N, the winter cell is 50% stronger than the symmetric cells, while the summer cell is half the strength of the symmetric cells. The latitude where the two cells meet is no longer the area of maximum vertical velocity; instead, it remains near the latitude of the heat source, as previously concluded by Lindzen and Hou (1988). When the heat source is located at 6° N, the winter cell dominates and it is more than four times as intense as the symmetric cells. In agreement with this, Zhang et al. (2008) found that all SMCs undergo marked seasonal cycles, with the one on the eastern Pacific peaking throughout the boreal fall.

The main goal of this article was to use observational and reanalysis data from different sources to add more observational evidence of the SRF over the ETPac, more specifically at Isla del Coco, located 495 km SSW of Cabo Blanco on the Nicoya Peninsula, Costa Rica (Lizano 2001).

MATERIALS AND METHODS

Year of Tropical Convection (YOTC) data

This paper used analysis from the Year of Tropical Convection (YOTC) research program (Waliser et al. 2012) to examine the relationship of SSTs, clouds, and low-level circulation features over the ETPac during the boreal summer, where the SMC has been previously observed. These data have a horizontal resolution of $0.5^\circ \times 0.5^\circ$, 15 vertical levels between 1,000 and 100 hPa and a temporal resolution of 6 h, from May 2008 through April 2010. We only considered analyses from the boreal summer of 2009, during which time the multivariate ENSO index (<https://psl.noaa.gov/enso/mei/>) ranged from 0.36 to 0.96, corresponding to weak warm anomalies over the ETPac. The agreement between ECMWF and QuikSCAT surface diver-

gence and vorticity analyses over the ETPac found by McNoldy et al. (2004), provided confidence that the ECMWF-based YOTC analyses were accurately depicting conditions over this region.

Pilot balloons data

Data gathered from the pilot balloons from the PACS-SONET project (Douglas and Murillo 2008) during May 1997 through January 1999 at Isla del Coco, Costa Rica, provided further information on the existence of the shallow return flow (SRF) near 5.5° N- 87° W (Alfaro 2008). Additional data were obtained from pilot balloons during a multidisciplinary research expedition in October 2007 and April 2008 (Cortés Núñez et al. 2009; Maldonado and Alfaro 2010).

ERA5

To compare the observational data to some statistical climatology, the reanalysis data from ERA5 (Hersbach et al. 2020) was used, which provided a spatial resolution of $0.25^{\circ} \times 0.25^{\circ}$, 37 vertical levels, with data from January 1979 to December 2020.

RESULTS

YOTC

Low clouds were usually found between the surface and 2 km, while high clouds were located above 8 km. Low-level trade winds from the southern hemisphere converged strongly with those of the northern hemisphere forming an ITCZ at approximately 10° N (Figure 1 A). High-level clouds were found near the average position of the ITCZ (low-level wind convergence), whereas low-level clouds were observed south of the ITCZ, including the southeastern Pacific, which corresponded to areas of maximum meridional low-level wind (Fig-

ure 1 B). Low-level convergence associated with the ITCZ in the ETPac was located between 2.5° N and 15° N, with maximum surface southerly winds between the equator and 5° N (Figure 2). These results were also consistent with those presented by Amador et al. (2006, 2016a, 2016b), Durán-Quezada et al. (2020), and with the QuikScat divergence patterns found by McNoldy et al. (2004) for 1999-2002 average values. The strongest values of low-level divergence were found between the equator and 2° N, with less well-defined convergence often occurring near 5° N, noting of course that the YOTC data sampled only a brief period during the transition from La Niña to El Niño. By July, the ITCZ was generally located between 8° N and 10° N, and it continued moving north until September, when it reached its northernmost position, often slightly north of 10° N (Figure 2). During summer months, cyclonic vorticity was present north of 8° N, zero relative vorticity near 7° N (white shading) and anticyclonic vorticity south of 7° N (Figure 3). Strong low-level southerly winds south of the ITCZ displayed magnitudes between 4 to 7 m s^{-1} (Figure 4), and started decreasing in magnitude and horizontal extent during October (not shown). Furthermore, Figure 4 is in agreement with the humidity convergence presented in Alfaro (2002). As part of the SMC, a shallow return flow (northerly winds) near the equator has been observed over the ETPac in the lowest 2-5 km of the atmosphere. To examine the characteristics of the SMC over this region in more detail, Figure 5 shows monthly averaged cross sections of YOTC meridional winds between 85° W and 95° W for the months of May, July and September 2009, respectively. Left panels, showing the full depth of the troposphere, revealed the traditional deep Hadley circulation with a stronger cross-equatorial cell and upper-level northerlies to the south of the ITCZ. To better reveal details of the lower-level SMC, the right panel of Figure 5 focus on the 1,000-600 hPa layer. As noted in earlier figures, low-level winds converged between 5° N and 10° N during these months. South of the ITCZ, low-level southerlies with peak speeds between 6

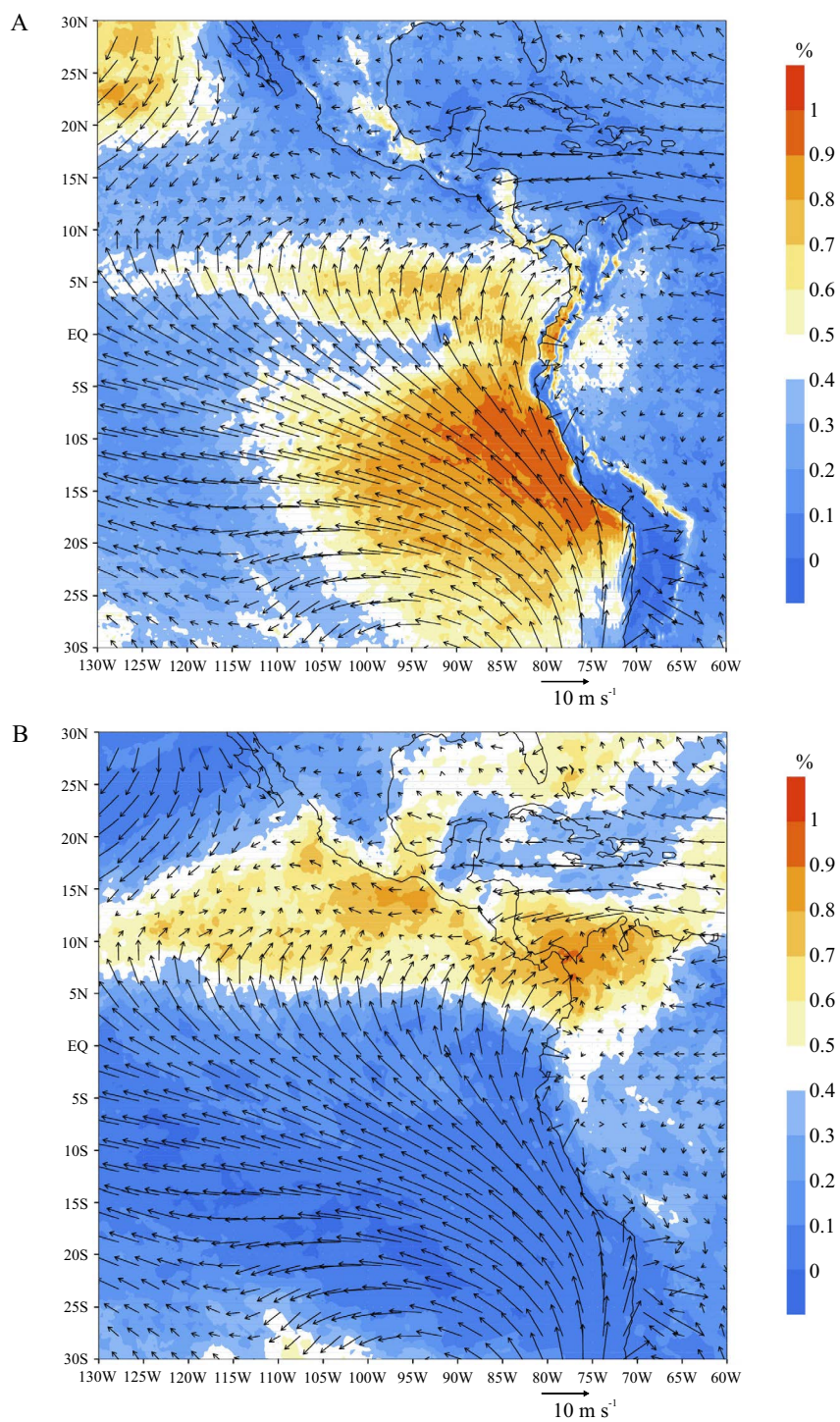


Figure 1. Fractional low and high-level cloud cover (scale on right) and surface wind (with the reference 10 m s⁻¹ vector shown at the bottom) for high level (A) and low level (B).

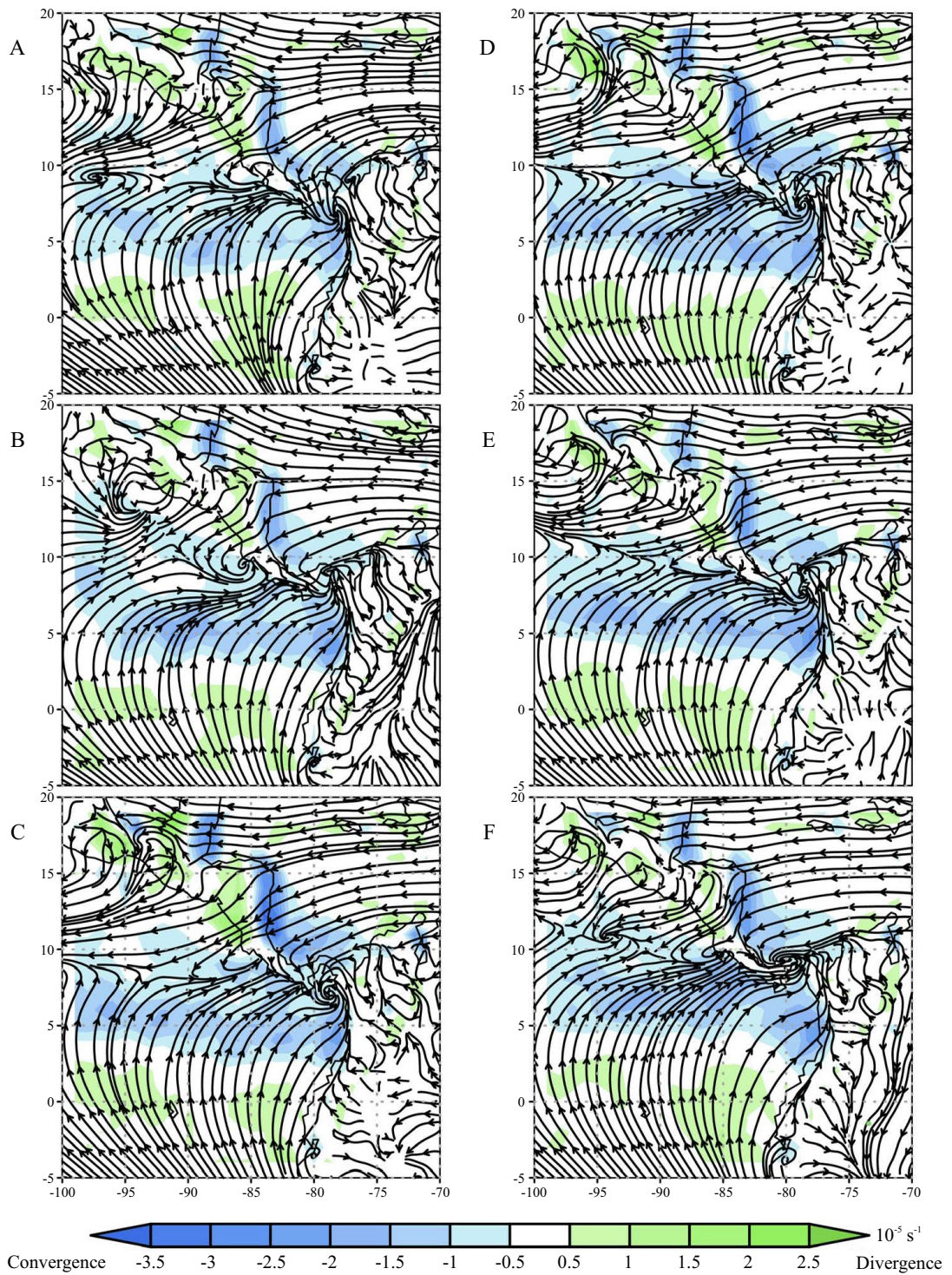


Figure 2. May-October 2009 divergence (10^{-5} s^{-1}) and streamlines at 1,000 hPa in sequence from A) to F).

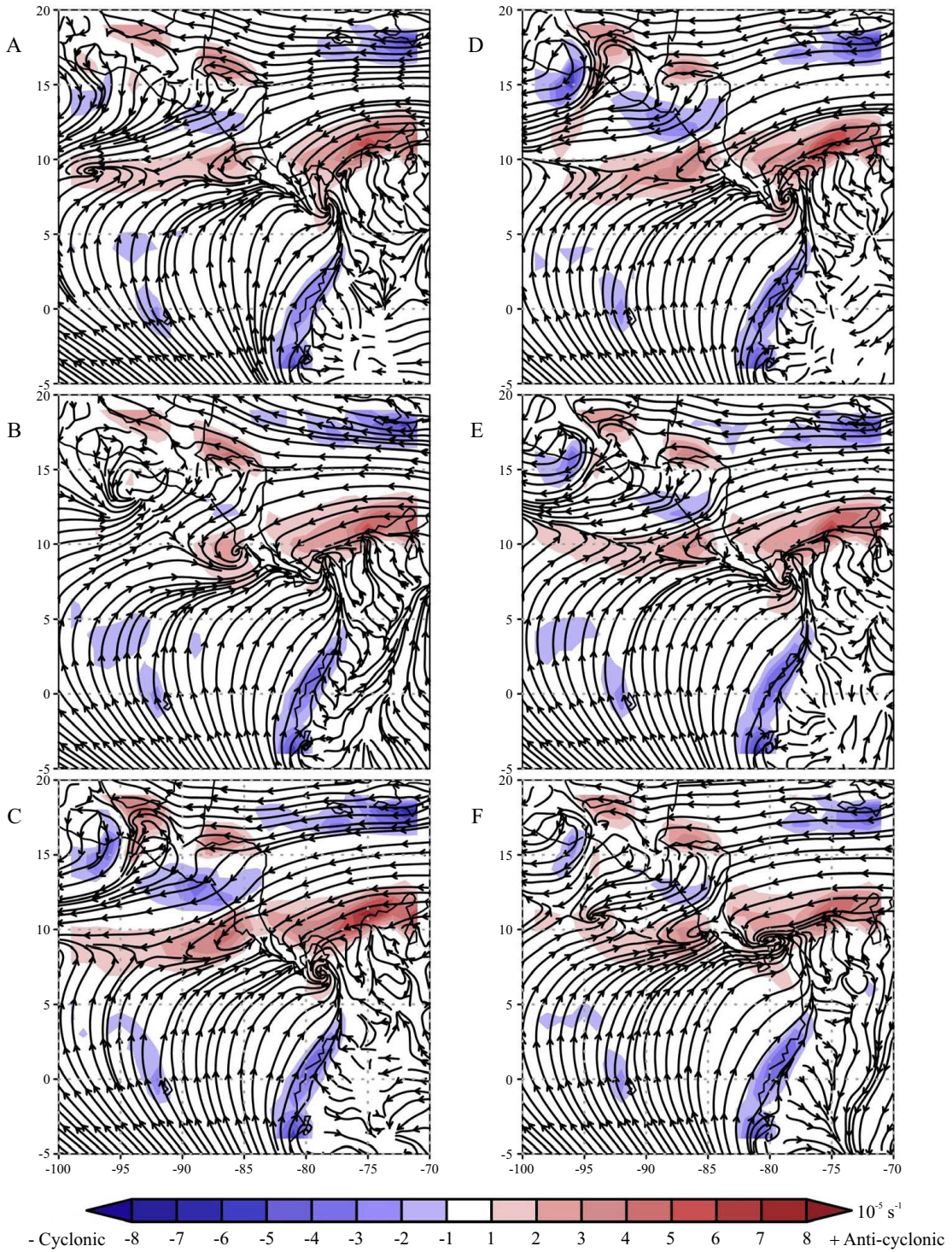


Figure 3. May-October 2009 vorticity (10^{-5} s^{-1}) and streamlines at 1,000 hPa in sequence from A) to F).

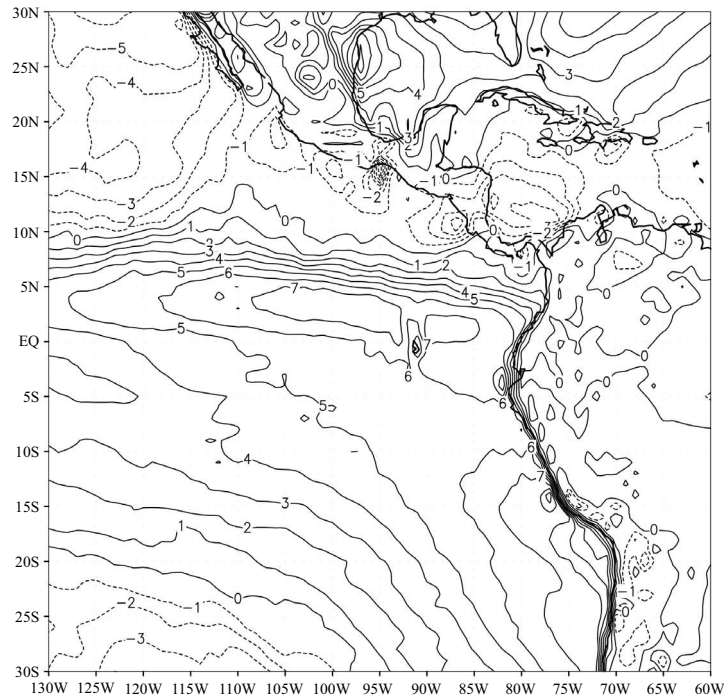


Figure 4. Meridional wind (m s^{-1}) at 1,000 hPa for July 2009.

and 7 m s^{-1} were observed within 20° S and 10° N . Atop this layer of southerly winds, a weak northerly ($1\text{--}2 \text{ m s}^{-1}$) return flow centered near 2.5° N was observed near the levels 800–700 hPa.

Some strengthening of the SMC between May and the later months was consistent with wind profiler observations from this region (Zhang et al. 2004). North of the ITCZ, low-level northerlies were present roughly between 10° N and 20° N , with no evidence of a shallow southerly return flow to the north. Note that the northerly maximum in July found near 12° N and 900 hPa could be partially a reflection of the Papagayo Jet (Chelton et al. 2000; Amador et al. 2006, 2016b; Mora-Rojas 2017; Durán-Quesada et al. 2020) which had a peak northerly component near 925 hPa.

Characteristics of the SMC, and in particular, the northerly return flow between 800 hPa and 700 hPa in the 2009 YOTC analyses were largely consistent with the ETPac observations of this flow presented in Zhang et al. (2004). With such con-

sistency between model analyses and observations, examining additional years of model analyses and interannual variability patterns would be helpful for understanding the variability of the SMC in this region.

Pilot balloons

Data from pilot balloons were analyzed at different vertical levels, and a southern shallow return flow was found over Isla del Coco (Figure 6). Vertical profiles of the meridional wind at mid-levels of the atmosphere during different months and years were observed (Figure 6 A). The layer where northerly winds can be located, varied in depth and maximum speed throughout the year, starting near 900 m ($\sim 910 \text{ hPa}$) and extending upwards to mid-levels near 5,000 m ($\sim 555 \text{ hPa}$). Peak speeds were found within 2,000 m ($\sim 800 \text{ hPa}$) and 3,000 m ($\sim 700 \text{ hPa}$). In more detail, it can be observed the spring meridional wind and the north-

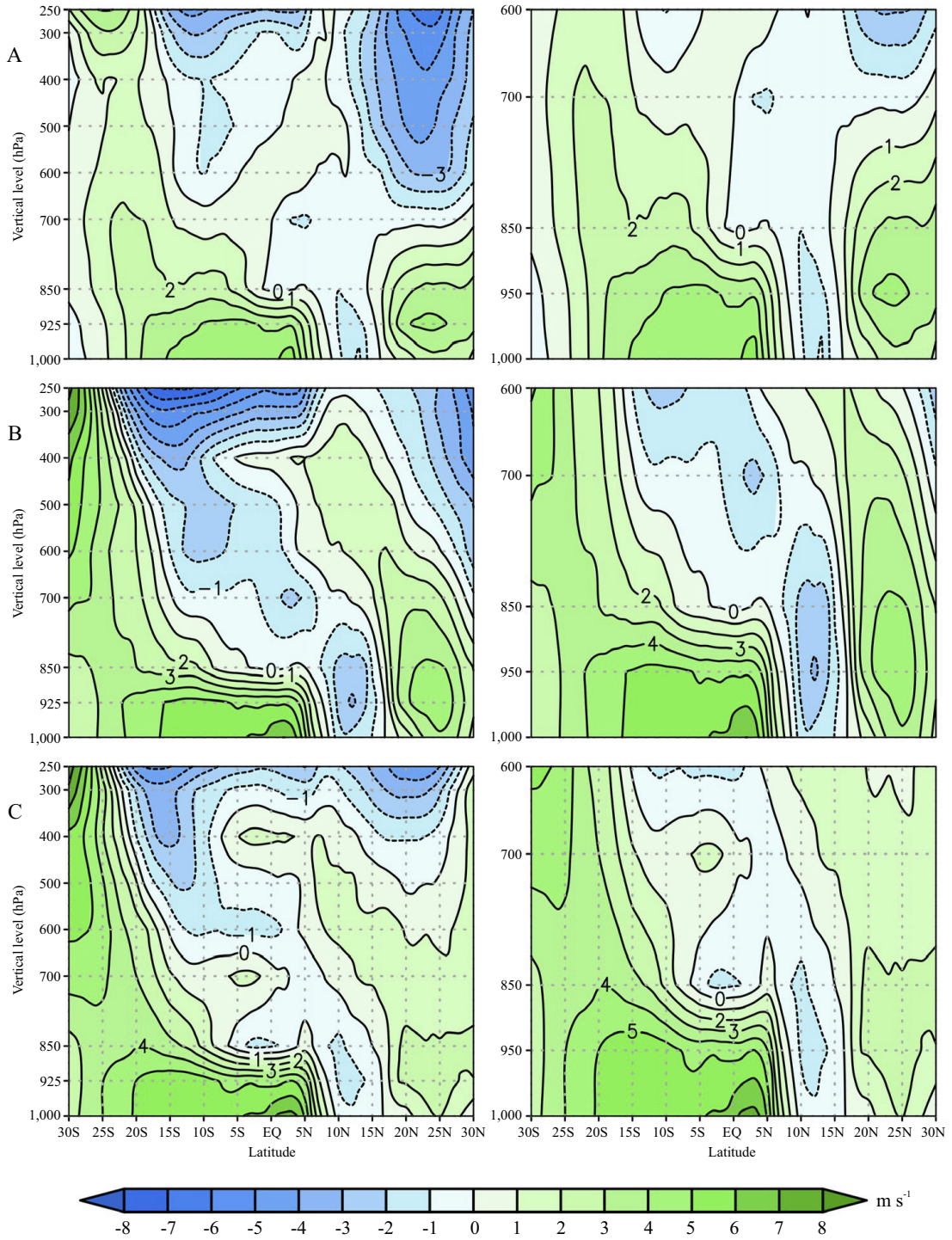


Figure 5. Meridional wind ($m s^{-1}$) cross section, averaged over the longitude range $5^{\circ} W-95^{\circ} W$ (YOTC) for May (A), July (B) and September (C). Left column shows the full depth of the troposphere whereas the right column shows from 1,000 to 600 hPa.

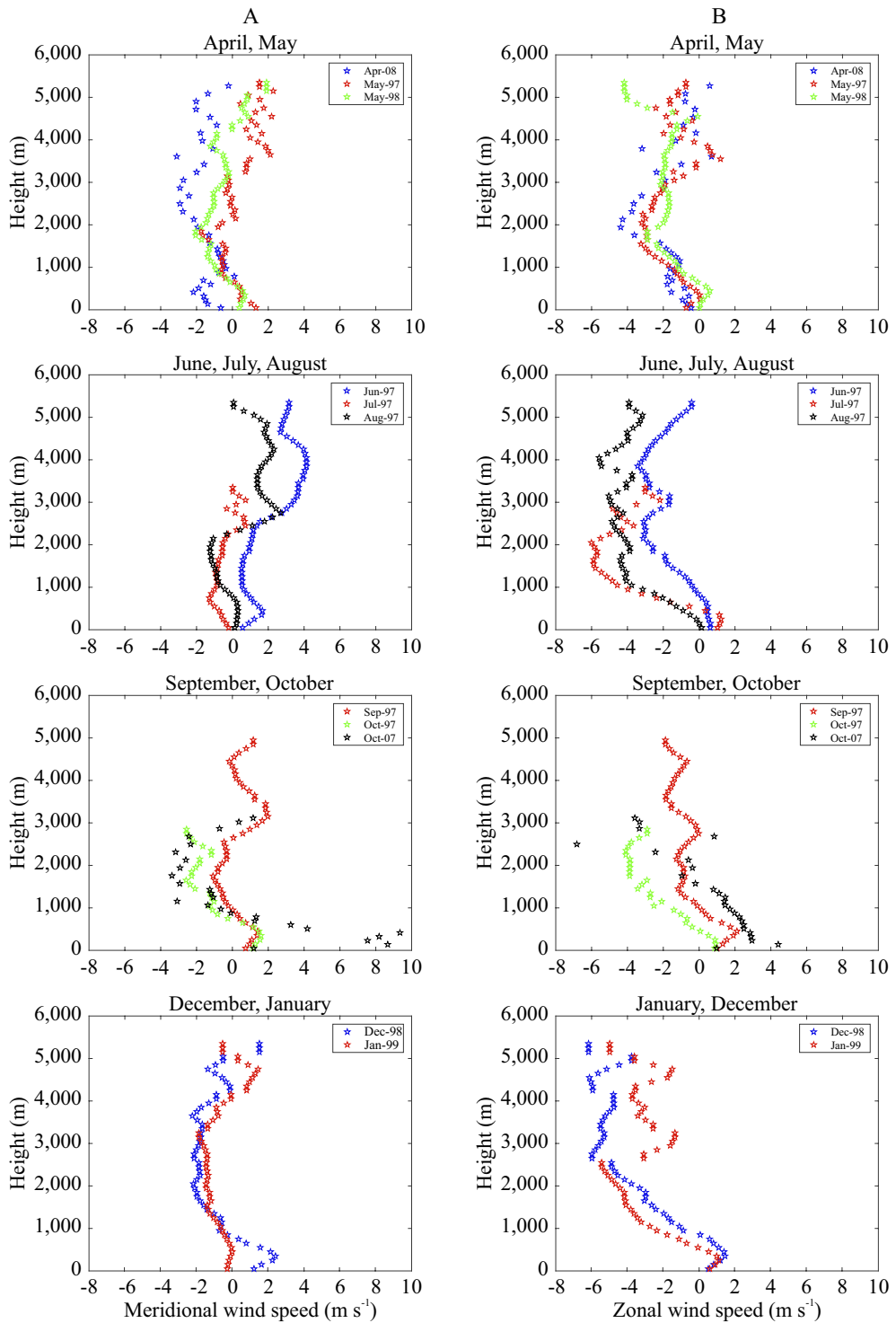


Figure 6. Meridional wind (A) and zonal wind (m s⁻¹) (B) at 5° N, 87° W from pilot balloons.

erly flow as negative wind from 900 m to approximately 3,500 m high (Figure 6). The return flow was not observed in June 1997; however, the SRF began to develop at lower levels again during July, and a stronger northerly flow was confined at lower levels in the fall, peaking at 3,000 m with an average speed of about 3 m s^{-1} , as well as a noticeable southerly flow above 3,000 m. These results were consistent with those presented by Maldonado and Alfaro (2010) and Alfaro (2008).

Westerly winds were found at low levels, consistent with the trade winds from the southern hemisphere curving north-eastward as they cross the equator, converging with trade winds from the northern hemisphere (Figure 6 B). At mid-levels over this region, a layer of easterly winds was found throughout most of the year, starting slightly below 1,000 m and extending upward to approximately 4,000 m through the spring and higher than 6,000 m through the summer. September and October displayed the lowest values of easterly winds, and the winter months showed a deeper layer of easterly winds with increasing height.

ERA5

The ERA5 data analysis showed the existence of a SMC in the ETPac as well, more specifically the southern SMC on the atmosphere aloft Isla del Coco. Shallow meridional cells often met at higher latitudes as the ITCZ moved northwards with seasons, this meant the SMC follows the heat source as this last one moved meridionally throughout the year (Figures 7-12), reaching its northernmost position during the boreal summer (except 2009) and shifting southwards during fall. The displacement of the shallow southern cell had a similar pattern, usually centered at lower latitudes during winter, and moving to higher latitudes as the ITCZ moved northwards with the seasons (except in 1997), reaching its maximum latitude during the boreal summer and moving southwards in fall as the ITCZ moved southwards again. Additional years should be incorporated to understand the variation of the

vertical level at which the SMC was centered, as this one ranged within 900 hPa and 810 hPa. During El Niño events, the southern cell tended to be centered at lower latitudes when compared to La Niña and neutral years. Moreover, the northern and southern SMCs met at lower latitudes during El Niño and at higher latitudes during La Niña.

Streamlines of meridional and vertical wind showed a well-defined circulation for most of the available years and seasons, i.e. 1997 (months March, June, September, December), 1998 (from May through December), 1999 (except for the months February, March, June), 2007 (for most part of the year, except in January), 2008 (for most of the year, except in February, March) and 2009 (June, September and November) (Figures 7-12).

DISCUSSION

Several authors have documented a SMC in the eastern tropical Pacific over the past 20 years, a low-level cell characterized by its own dynamics. This cell is embedded in the well-known Hadley circulation on each hemisphere, although they are not zonally nor meridionally symmetric cells and are not found continuously all around the globe, instead these cells have been observed and modeled as localized cells at certain longitudes. Some authors have formulated the formation and maintenance of the SMC as a sea-breeze-type circulation, without considering the latitudinal variation of the Coriolis parameter. Other studies simulated heat sources at the equator and nearby to observe the consequent circulation at low levels of the atmosphere, finding symmetric cells when the heat source is located at the equator. According to the simulations, a stronger and more organized SMC is observed on the winter hemisphere, with strong inflow at low levels and a weak-but almost permanent-return flow at mid-levels of the atmosphere. Moreover, the latitude where the two cells meet remains close to the heat source. However, the lat-

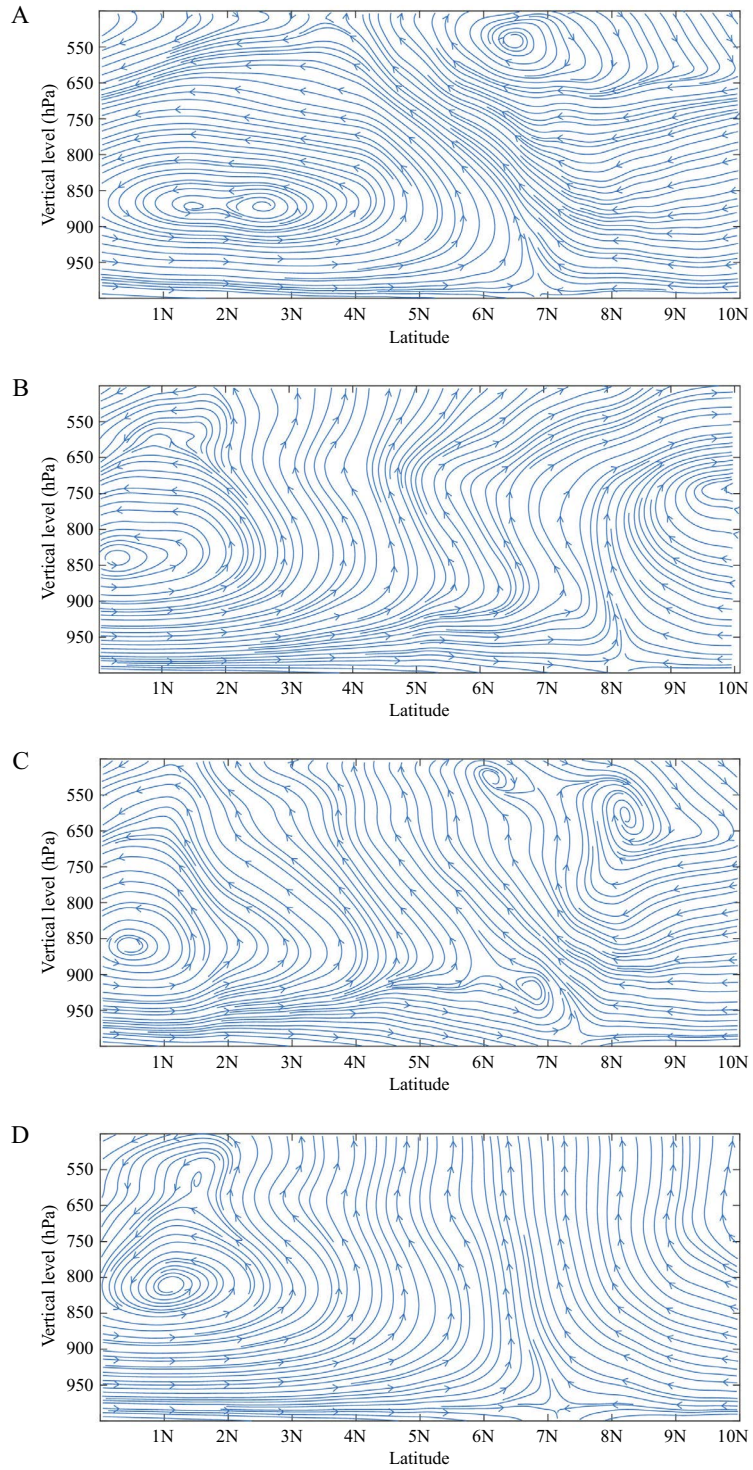


Figure 7. Streamlines, cross sections in 1997, 87° W. A) Winter. B) Summer. C) Spring. D) Fall.

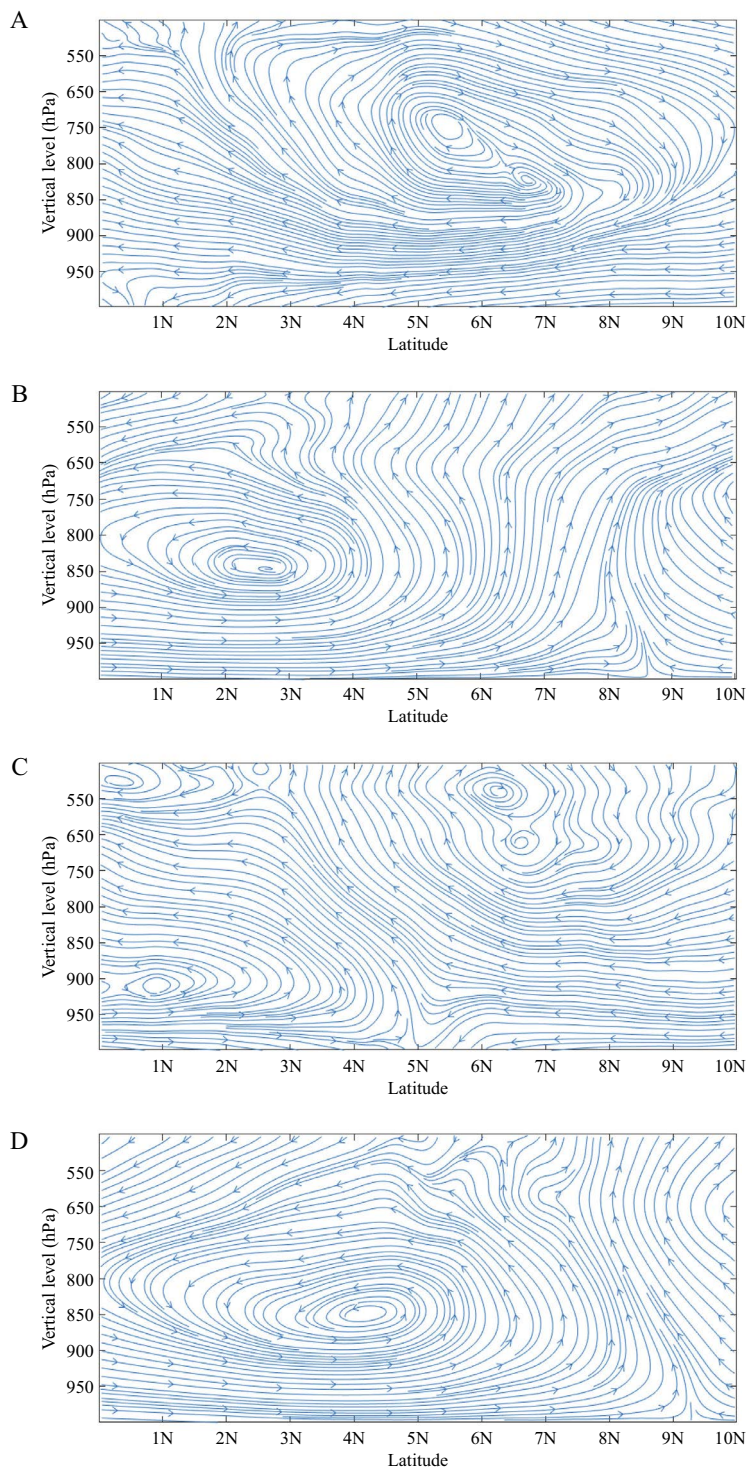


Figure 8. Streamlines, cross sections in 1998, 87° W. A) Winter. B) Summer. C) Spring. D) Fall.

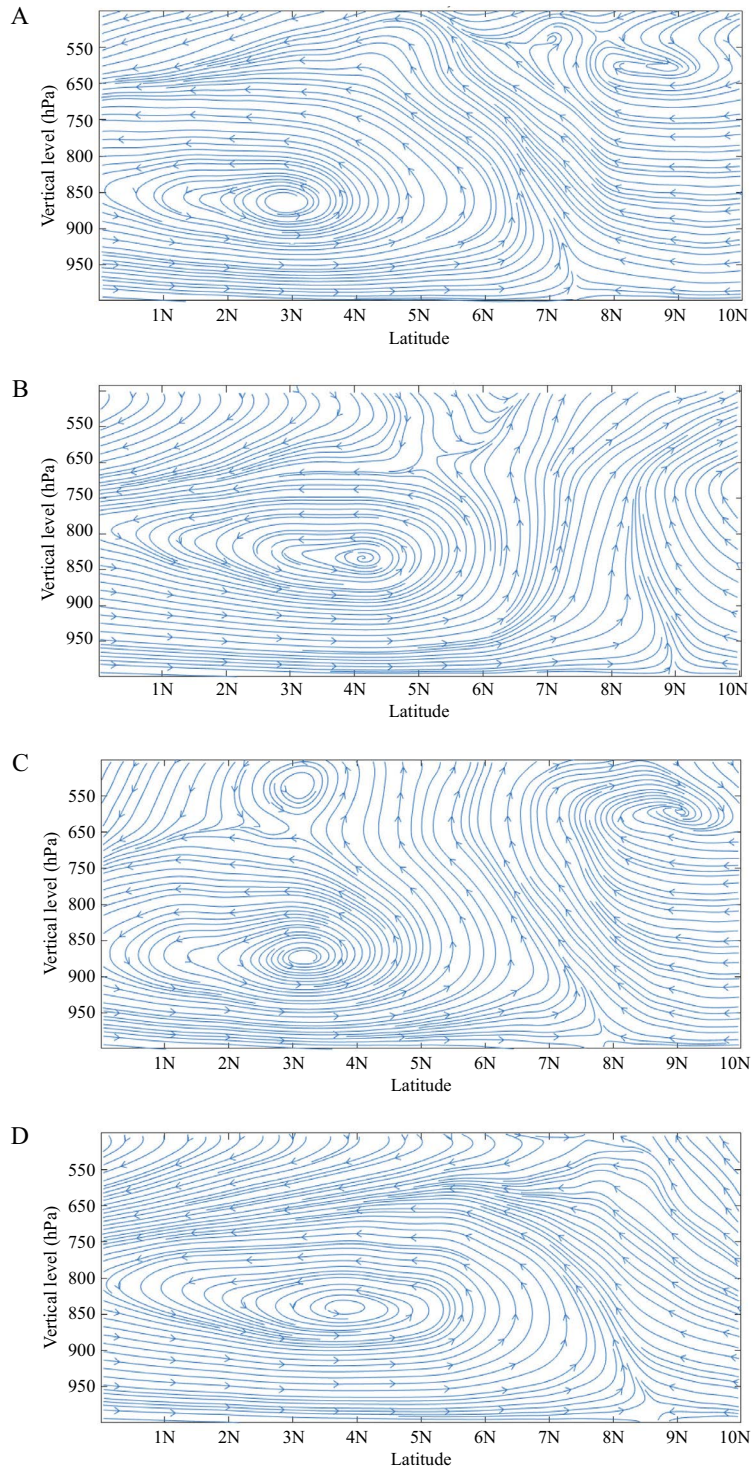


Figure 9. Streamlines, cross sections in 1999, 87° W. A) Winter. B) Summer. C) Spring. D) Fall.

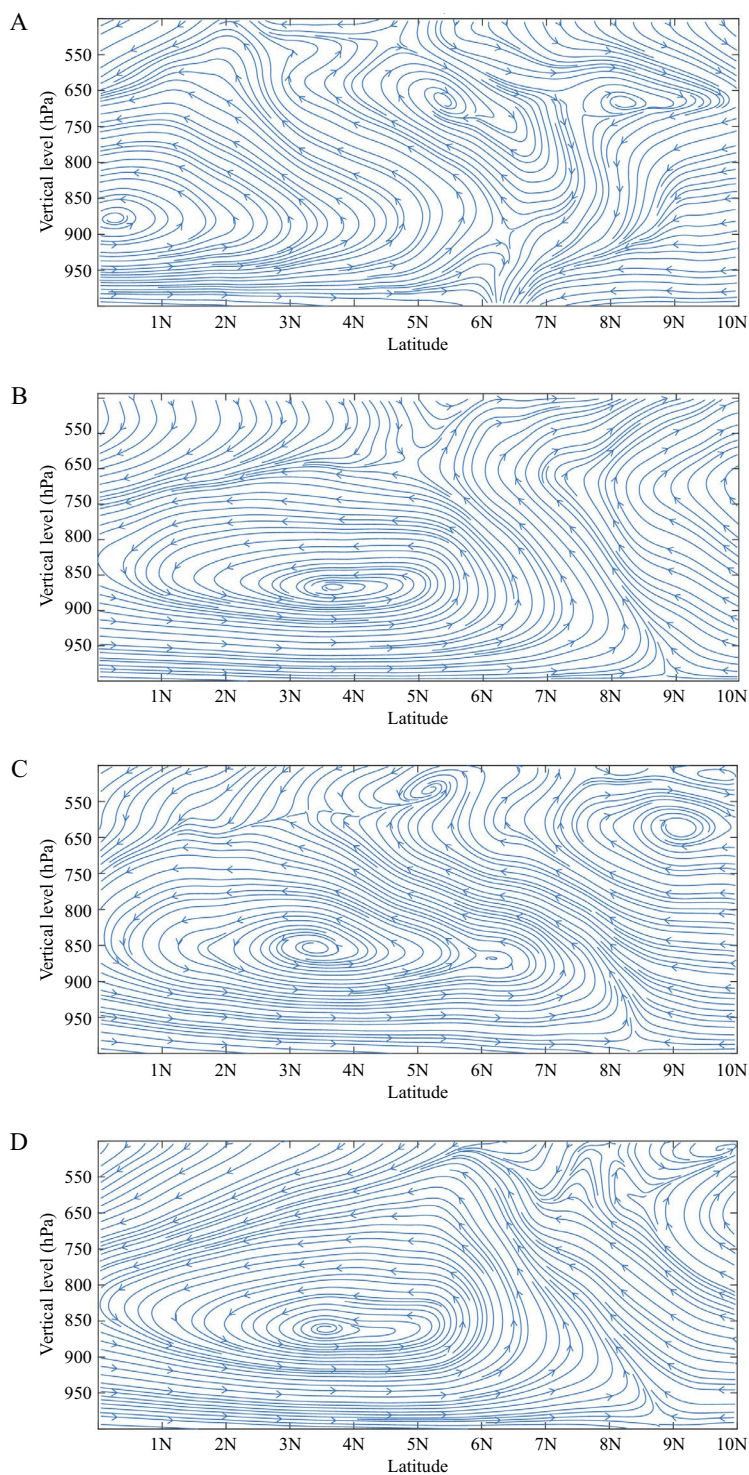


Figure 10. Streamlines, cross sections in 2007, 87° W. A) Winter. B) Summer. C) Spring. D) Fall.

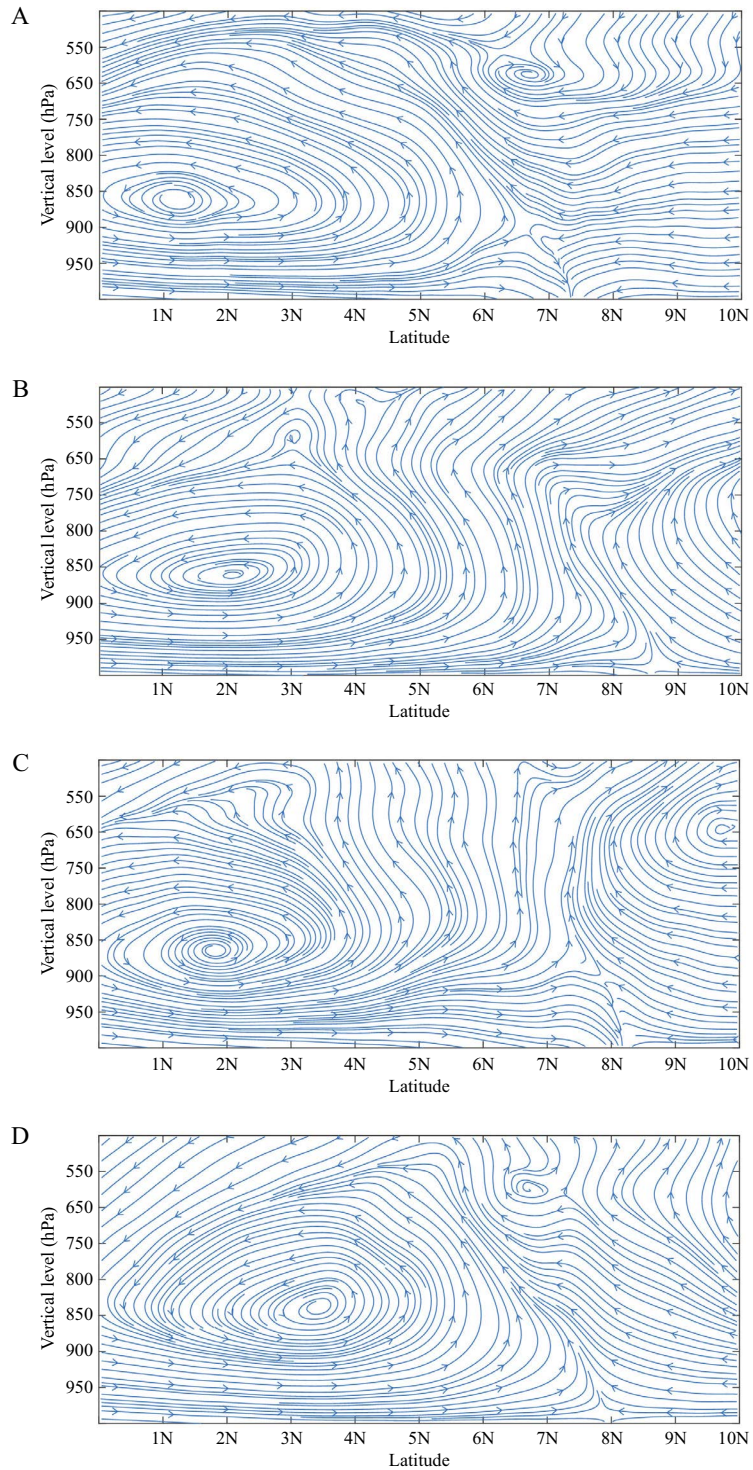


Figure 11. Streamlines, cross sections in 2008, 87° W. A) Winter. B) Summer. C) Spring. D) Fall.

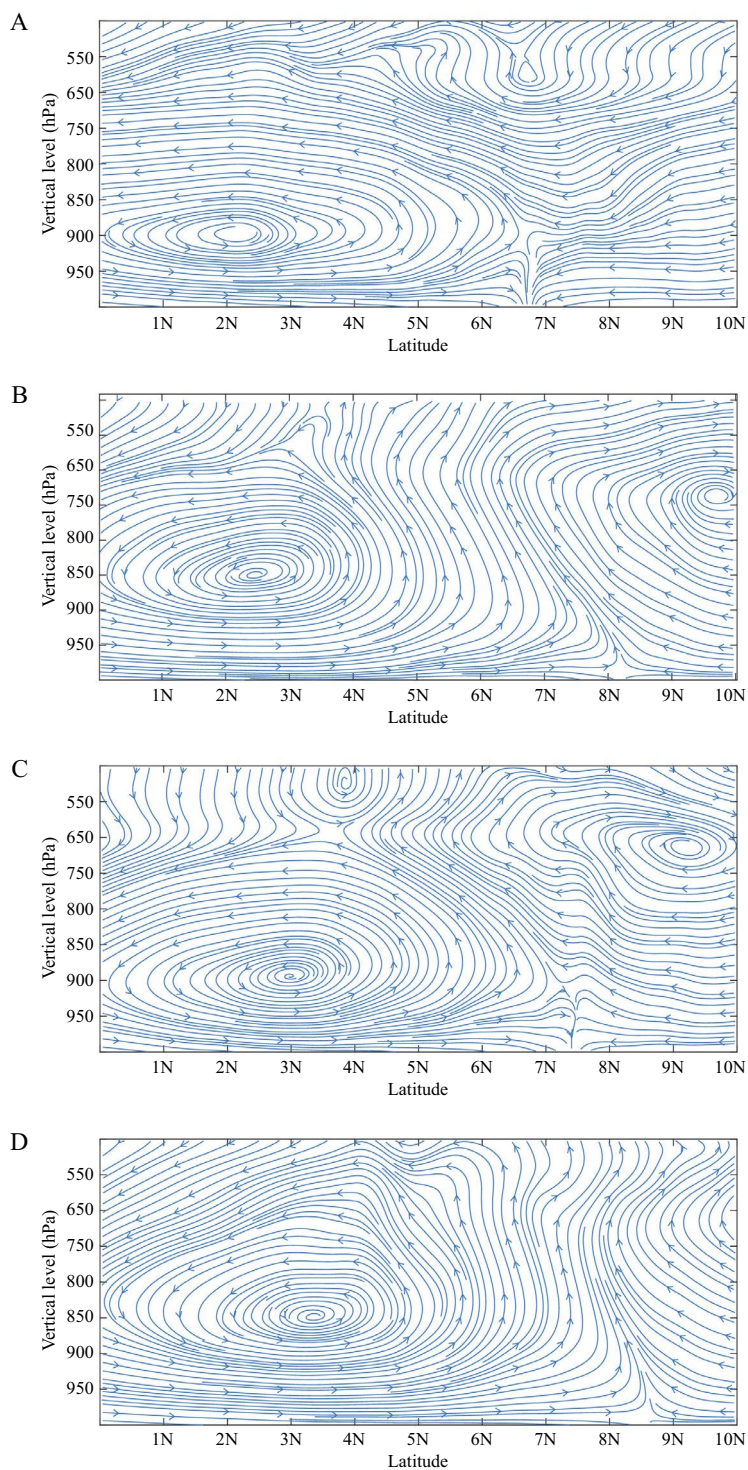


Figure 12. Streamlines, cross sections in 2009, 87° W. A) Winter. B) Summer. C) Spring. D) Fall.

itude of maximum ascending motion behaves in a different manner, as it does not always match the latitude of the heat source.

This SMC in the eastern tropical Pacific has been observed in data from different sources, e.g. from the reanalysis ERA5 to real data, such as the one gathered from pilot balloons. Our results showed that this meridional circulation near 87° W, where Isla del Coco is located, with a latitudinal coverage ranging from 0 to 4° N and its strongest activity, occurs at levels within 900 hPa to 700 hPa. This SMC is located close to the equator during warm episodes of ENSO, while for cold and neutral events, it is located further north of the equator. The most intense and organized SMC was found during the boreal summer and fall, consistent with a strong austral winter and spring cell, respectively. In the vertical meridional wind profile analysis, a northerly return flow was observed at low and mid-levels of the atmosphere for most of the year (2009). This northerly flow was particularly noticeable from 900 m (~ 910 hPa) to 5,000 m (~ 555 hPa), peaking within 2,000 m (~ 800 hPa) and 3,000 m (~ 700 hPa).

The Year of Tropical Convection wind data from 2009 was used to construct another vertical profile of the meridional wind in that region, and a shallow return flow was found as well, located at low levels of the atmosphere. Southerly winds at surface levels contrast with the northerly return flow at mid-levels of the atmosphere just aloft. The low-level southerly winds flow from 20° S to 10° N, converging from 5° N to 10° N during May, July and September and reaching peak speeds of 6 to 7 m s^{-1} . The northerly flow is not as strong as the surface flow, ranging from 1 to 2 m s^{-1} , and it is usually centered at approximately 2.5° N, within 850 hPa and 700 hPa, depending on the month. Another feature evidencing the SMC is the stratocumulus clouds found north and south of the equator, suggesting that shallow convection occurs in that area. Philander et al. (1996) pointed it out that thin layers of stratus clouds develop in regions of subsidence where the surface winds evaporate

water vapor from the ocean. A strong low-level atmospheric inversion traps this moist air forming stratus clouds at the base of the inversion. Most of the data from the reanalysis ERA5 displays a clear and persistent pattern of a SMC with variable latitudinal position, as it migrates with the seasonal migration of the ITCZ: northward during the boreal spring and summer, and southward during fall and winter. In the fall season, the cell is stronger than the one found in the summer season, and by winter the cell is centered at the lowest latitudes, almost near the equator. Another interesting result from the reanalysis ERA5 was that the cell is centered at lower latitudes during El Niño events due to the warmer temperatures found at lower latitudes. The latitude where both cells converge was found at lower latitudes during El Niño events as well, in contrast with its position during La Niña and neutral events.

Results from this study agree with some of the previously modeled mechanisms for the generation of a shallow meridional circulation, discussed in the introduction. A simulated diabatic heat source at the Chocó region has been tested in recent years (Mesa-Sánchez and Rojo-Hernández 2020) to reproduce the large-scale circulation in Meso-America and the northern area of South America. A resulting Rossby wave seems to be responsible for part of the dynamics of the low-level circulation south of the ITCZ, as this wave generates two vortices west of the heating source, explaining the westerly winds converging at the heating source. Our data evidenced these westerly winds at low levels of Isla del Coco. The SMC is embedded in the southwestern cyclone, which is weaker than the northwestern one.

Easterly waves moving within the ITCZ have also been identified (Huaman et al. 2021) as a mechanism for explaining the low-level circulation, clouds and convection observed in this region during the authors research experiment. The cyclonic part of the tropical wave enhances intense convective activity at the ITCZ, and the anticyclonic part of the tropical wave does not allow for deep

convection, producing and enhancing the SMC and the shallow convection south of the ITCZ.

Results from this study show a complex pattern of the SMC at the eastern tropical Pacific, which seems to be more likely associated to the superposition of signals, from transitory disturbances (easterly waves) of different time scales interacting with the ITCZ, to the already recognized diabatic heating ‘pulses’ associated to the enormous latent heat released in the Choco region, producing ‘pulses’ of Ekman pumping and a Rossby wave pattern around the heat source. Additional studies should be conducted toward the understanding of the implications for the weather and climate at this island.

ACKNOWLEDGMENTS

This research was funded by the University of Costa Rica projects: B9454 (VI-Grupos), C2103, A5719, B0810, A1715, C2806, A4906, B8604, C0130, C2766 (IBWOCLIMA), C3195. Authors thank to the UCR School of Physics for giving us the research time to develop this study and to the UCR research centers CIGEFI, CINPA and CIMAR for their logistic support during the data compilation and analysis.

Declaration of interest

The authors have nothing to declare.

Author contributions

Gabriela Mora-Rojas: conceptualization, methodology, software, validation, formal analysis, investigation, resources, data curation, writing-original draft, writing-review and editing, visualization, supervision, project administration, funding acquisition. Eric J. Alfaro: conceptualization, formal analysis, investigation, resources, data curation, writing-review and editing, funding acquisition.

REFERENCES

- ALFARO E. 2002. Some characteristics of the annual precipitation cycle in Central America and their relationships with its surrounding tropical oceans. *Top Meteorol Oceanogr.* 9 (2): 88-103.
- ALFARO EJ. 2008. Ciclo diario y anual de variables troposféricas y oceánicas en la Isla del Coco, Costa Rica. *Rev Biol Trop.* 56 (2): 19-29. DOI: <https://doi.org/10.15517/rbt.v56i2.26936>
- AMADOR JA, ALFARO EJ, LIZANO OG, MAGAÑA VO. 2006. Atmospheric forcing of the eastern tropical Pacific: a review. *Prog Oceanogr.* 69: 101-142. DOI: <https://doi.org/10.1016/j.pcean.2006.03.007>
- AMADOR JA, DURÁN-QUESADA AM, RIVERA ER, MORA G, SÁENZ F, CALDERÓN B, MORA N. 2016b. The easternmost tropical Pacific. Part II: seasonal and intraseasonal modes of atmospheric variability. *Rev Biol Trop.* 64 (1): 23-57. DOI: <https://doi.org/10.15517/rbt.v64i1.23409>
- AMADOR JA, RIVERA ER, DURÁN-QUESADA AM, MORA G, SÁENZ F, CALDERÓN B, MORA N. 2016a. The easternmost tropical Pacific. Part I: a climate review. *Rev Biol Trop.* 64 (1): 1-22. DOI: <https://doi.org/10.15517/rbt.v64i1.23407>
- BACK LE, BRETHERTON CS. 2009. On the relationship between SST gradients, boundary layer winds and convergence over the tropical oceans. *J Clim.* 22: 4182-4196. DOI: <https://doi.org/10.1175/2009JCLI2392.1>
- CHELTON DB, ESBENSEN SK, SCHLAX MG, THUM N, FREILICH MH, WENTZ FJ, GENTEMANN CL, MCPHADEN MJ, SCHOPF PS. 2001. Observations of coupling between surface wind stress and sea surface temperature in the Eastern Tropical Pacific. *J Clim.* 14: 1479-1498. DOI: [https://doi.org/10.1175/1520-0442\(2001\)014<1479:OOCBSW>2.0.CO;2](https://doi.org/10.1175/1520-0442(2001)014<1479:OOCBSW>2.0.CO;2)
- CHELTON DB, FREILICH MH, ESBENSEN SK. 2000. Satellite observations of the wind jets off the Pacific coast of Central America. Part II: re-

- gional relationships and dynamical considerations. *Mon Weather Rev.* 128: 1993-2018. DOI: [https://doi.org/10.1175/1520-0493\(2000\)128<2019:SOOTWJ>2.0.CO;2](https://doi.org/10.1175/1520-0493(2000)128<2019:SOOTWJ>2.0.CO;2)
- CORTÉS NÚÑEZ J, ACUÑA GONZÁLEZ J, ALFARO MARTÍNEZ E, LIZANO RODRÍGUEZ O, MORALES RAMÍREZ Á. 2009. Conocimiento y gestión de medios marinos y coralinos del Area de Conservación Marina Isla del Coco. Informe final del proyecto de investigación No. 08-A7-520. San José: Centro de Investigación en Ciencias del Mar y Limnología (CIMAR). [accessed 2023 Jul]. <http://www.kerwa.ucr.ac.cr/handle/10669/436>.
- DESER C, BATES JJ, WAHL S. 1993. The influence of sea surface temperature gradients on stratiform cloudiness along the equatorial front in the Pacific Ocean. *J Clim.* 6: 1172-1179. DOI: [https://doi.org/10.1175/1520-0442\(1993\)006<1172:TIOSST>2.0.CO;2](https://doi.org/10.1175/1520-0442(1993)006<1172:TIOSST>2.0.CO;2)
- DE SZOEKE SP, BRETHERTON CS, BOND NA, CRONIN MF, MORLEY BM. 2005. EPIC 95°W observations of the Eastern Pacific atmospheric boundary layer from the cold tongue to the ITCZ. *J Atmos Sci.* 62: 426-442. DOI: <https://doi.org/10.1175/JAS-3381.1>
- DOUGLAS MW, MURILLO J. 2008. The Pan-American climate studies sounding network. *Bull Am Meteorol Soc.* 89: 1709-1726. DOI: <https://doi.org/10.1175/2008BAMS2521.1>
- DURÁN-QUESADA AM, SORÍ R, ORDÓÑEZ P, GIMENO L. 2020. Climate perspectives in the Intra-Americas seas. *Atmosphere.* 11 (9): 959. DOI: <https://doi.org/10.3390/atmos11090959>
- GONZÁLEZ AO, MORA-ROJAS G. 2014. Balanced dynamics of deep and shallow Hadley circulations in the tropics. *J Adv Model Earth Syst.* 6: 777-804. DOI: <https://doi.org/10.1002/2013MS000278>
- HACK JJ, SCHUBERT WH. 1990. Some dynamical properties of idealized, thermally-forced meridional circulations in the Tropics. *Meteorol Atmos Phys.* 44: 101-117. DOI: <https://doi.org/10.1007/BF01026813>
- HACK JJ, SCHUBERT WH, STEVENS DE, KUO HC. 1989. Response of the Hadley circulation to convective forcing in the ITCZ. *J Atmos Sci.* 46: 2957-2973. DOI: [https://doi.org/10.1175/1520-0469\(1989\)046<2957:ROTHCT>2.0.CO;2](https://doi.org/10.1175/1520-0469(1989)046<2957:ROTHCT>2.0.CO;2)
- HERSBACH H, BELL B, BERRISFORD P, HIRAHARA S, HORÁNYI A, MUÑOZ-SABATER J, NICOLAS J, PEUBEY C, RADU R, SCHEPERS D, et al. 2020. The ERA5 global reanalysis. *Q J R Meteorol Soc.* 146: 1999-2049. DOI: <https://doi.org/10.1002/qj.3803>
- HUAMAN L, MALONEY ED, SHUMACHER C, KALIDIS GN. 2021. Easterly waves in the East Pacific during OTREC 2019 field campaign. *J Atmos Sci.* 78 (12): 4071-4088. DOI: <https://doi.org/10.1175/JAS-D-21-0128.1>
- KANG SM, HELD IM, FRIERSON DMW, ZHAO M. 2008. The response of the ITCZ to extratropical thermal forcing: idealized slab-ocean experiments with a GCM. *J Clim.* 21: 3521-3532. DOI: <https://doi.org/10.1175/2007JCLI2146.1>
- LINDZEN RS, HOU AV. 1988. Hadley circulations for zonally averaged heating centered off the Equator. *J Atmos Sci.* 45: 2416-2427. DOI: [https://doi.org/10.1175/1520-0469\(1988\)045<2416:HCFZAH>2.0.CO;2](https://doi.org/10.1175/1520-0469(1988)045<2416:HCFZAH>2.0.CO;2)
- LINDZEN RS, NIGAM S. 1987. On the role of sea surface temperature gradients in forcing low-level winds and convergence in the tropics. *J Atmos Sci.* 44: 2418-2436. DOI: [https://doi.org/10.1175/1520-0469\(1987\)044<2418:OTROSS>2.0.CO;2](https://doi.org/10.1175/1520-0469(1987)044<2418:OTROSS>2.0.CO;2)
- LIZANO O. 2001. Batimetría de la plataforma insular alrededor de la Isla del Coco, Costa Rica. *Rev Biol Trop.* 49 (2): 163-170.
- MALDONADO T, ALFARO E. 2010. Comparación de las salidas del modelo MM5v3 con datos observados en la Isla del Coco, Costa Rica. *Tecnol Marcha.* 23 (4): 3-28.
- MCGAULEY M, ZHANG C, BOND NA. 2004. Large-scale characteristics of the atmospheric boundary layer in the Eastern Pacific cold tongue-ITCZ region. *J Clim.* 17: 3907-3920. DOI: <https://doi.org/10.1175/1520->

- 0442(2004)017<3907:LCOTAB>2.0.CO;2
McNOLDY BD, CIESIELSKI PE, SCHUBERT WH, JOHNSON RH. 2004. Surface winds, divergence, and vorticity in stratocumulus regions using QuikSCAT and reanalysis winds. *Geophys Res Lett.* 31: L08105. DOI: <https://doi.org/10.1029/2004GL019768>
- MESA-SÁNCHEZ OL, ROJO-HERNÁNDEZ JD. 2020. On the general circulation of the atmosphere around Colombia. *Rev Acad Colomb Cienc Exactas Fis Nat.* 44 (172): 857-875. DOI: <https://doi.org/10.18257/raccefyn.899>
- MORA-ROJAS G. 2017. Climatology of the low-level winds over the intra-Americas sea using satellite and reanalysis data. *Top Meteorol Oceanogr.* 16 (1): 15-30. <https://www.kerwa.ucr.ac.cr/handle/10669/76016>.
- NEIBURGER M, JOHNSON D, CHIEN C. 1961. Studies of the structure of the atmosphere over the eastern Pacific Ocean in summer, I. The inversion over the eastern north Pacific Ocean. *Univ Calif Press Publ Meteorol.* 1: 1-94.
- NOLAN DS, POWELL SW, ZHANG C, MAPES BE. 2010. Idealized simulations of the Intertropical Convergence Zone and its multilevel flows. *J Atmos Sci.* 67: 4028-4053. DOI: <https://doi.org/10.1175/2010JAS3417.1>
- NOLAN DS, ZHANG C, CHEN S. 2007. Dynamics of the shallow meridional circulation around Intertropical Convergence Zones. *J Atmos Sci.* 64: 2262-2285. DOI: <https://doi.org/10.1175/JAS3964.1>
- PHILANDER SGH, GU D, HALPERN D, LAMBERT G, LI T, HALPERN D, LAU NC, PACANOWSKI RC. 1996. Why is the ITCZ mostly north of the Equator. *J Clim.* 9: 2958-2972. DOI: [https://doi.org/10.1175/1520-0442\(1996\)009<2958:WTII MN>2.0.CO;2](https://doi.org/10.1175/1520-0442(1996)009<2958:WTII MN>2.0.CO;2)
- SCHUBERT WH, CIESIELSKI PE, STEVENS DE, KUO H. 1991. Potential vorticity modeling of the ITCZ and the Hadley circulation. *J Atmos Sci.* 48: 1493-1509. DOI: [https://doi.org/10.1175/1520-0469\(1991\)048<1493:PVMOTI>2.0.CO;2](https://doi.org/10.1175/1520-0469(1991)048<1493:PVMOTI>2.0.CO;2)
- TOMAS RA, WEBSTER PJ. 1997. The role of inertial instability in determining the location and strength of near-equatorial convection. *Q J R Meteorol Soc.* 123 (542): 1445-1482. DOI: <https://doi.org/10.1002/qj.49712354202>
- TRENBERTH KE, STEPANIAK DP, CARON JM. 2000. The global monsoon as seen through the divergent atmospheric circulation. *J Clim.* 13: 3969-3993. DOI: [https://doi.org/10.1175/1520-0442\(2000\)013<3969:TGMAST>2.0.CO;2](https://doi.org/10.1175/1520-0442(2000)013<3969:TGMAST>2.0.CO;2)
- VON FICKER H. 1936. Die Passatinversion. *Veröff Meteor Inst Univ Berlin.* 1: 1-33.
- WALISER DE, MONCRIEFF MW, BURRIDGE D, FINK AH, GOCHIS D, GOSWAMI BN, GUAN B, HARR P, HEMING J, HSU H, et al. 2012. The “Year” of Tropical Convection (May 2008-April 2010): climate variability and weather highlights. *Bull Am Meteorol Soc.* 93: 1189-1218. DOI: <https://doi.org/10.1175/2011BAMS3095.1>
- WALLACE JM, MITCHELL TP, DESER C. 1989. The influence of sea-surface temperature on surface wind in the Eastern Equatorial Pacific: seasonal and interannual variability. *J Clim.* 2: 1492-1499. DOI: [https://doi.org/10.1175/1520-0442\(1989\)002<1492:TIOSST>2.0.CO;2](https://doi.org/10.1175/1520-0442(1989)002<1492:TIOSST>2.0.CO;2)
- WANG Y, XIE S, WANG B, XU H. 2005. Large-scale atmospheric forcing by southeast Pacific boundary layer clouds: a regional model study. *J Clim.* 18: 934-951. DOI: <https://doi.org/10.1175/JCLI3302.1>
- ZHANG C, MCGAULEY M, BOND NA. 2004. Shallow meridional circulation in the tropical eastern Pacific. *J Clim.* 17: 133-139. DOI: [https://doi.org/10.1175/1520-0442\(2004\)017<0133:SMCITT>2.0.CO;2](https://doi.org/10.1175/1520-0442(2004)017<0133:SMCITT>2.0.CO;2)
- ZHANG C, NOLAN DS, THORNCROFT CD, NGUYEN H. 2008. Shallow meridional circulations in the tropical atmosphere. *J Clim.* 21: 3453-3470. DOI: <https://doi.org/10.1175/2007JCLI1870.1>